Calculation of pair production by photons of energies near threshold on atoms

H. K. Tseng
Department of Physics, National Central University, Chung-Li, Taiwan 32054, Republic of China
(Received 29 December 1993)

We calculated numerically in a relativistic partial-wave formulation the positron energy spectra of pair-production $\sigma(E_+)$ in the field of atoms with atomic number $Z=1$, 6, 13, and 82 for photons of energies near threshold, $k=2.001$, 2.01, and 2.10 m_ec^2, where E_+ is the positron energy. Our results indicate that in this low-photon-energy region, the atomic-electron screening effect increases as Z increases, k decreases, and E_+ decreases. The ratio of screened to point-Coulomb cross sections $\sigma(E_+)$ varies from 0.985 to 1.69×10^4. When the screening effect is important, it increases the cross section $\sigma(E_+)$. Our results also indicate that the approximate treatment of screening through energy-shift screening theory becomes inadequate when the screening effect is very important. The approximate treatment of screening through the corrected-effective normalization screening theory works fine in this low-photon-energy region, except for the case with $Z=6$, $k=2.001m_ec^2$, and $E_+=1.0001m_ec^2$, where the screening effect is not a normalization effect.

PACS number(s): 32.80.−t, 32.90.+a, 32.80.Cy

With the continuing improvements in computers it is becoming feasible to make fairly accurate theoretical calculations of pair-production cross sections by low-energy photons on atoms. Extensive point-Coulomb results from near threshold to 5 MeV have been given by Øverbø, Mork, and Olsen (ØMO) [1], using a method similar to that of Jaeger and Hulme [2]. By using the corrected-effective normalization screening theory (CNST) and the energy-shift screening theory (EST) for the atomic-electron screening effect, Tseng and Pratt [3] have converted all the point-Coulomb results of ØMO to the screened results for incident-photon energies in the range $(2.10-10.0)m_ec^2$. These results are in good agreement with experiments [3,4]. As we know, the atomic-electron screening effect on pair-production cross sections becomes more important as the incident photon energy decreases. Can the CNST and EST be used for lower photon energies? We wish to report results on the cross section of pair production by photons of energies k from $2.10m_ec^2$ down to $2.001m_ec^2$, obtained with a direct numerical calculations by using an exact relativistic partial-wave formulation. In this work we describe our basic process as the single-photon production of electron-positron pairs from an unpolarized isolated atom. In addition, we use a simplified model which is adequate for a wide range of atoms and the process at the kinetic energy of the created electron (or positron) above the keV range [5]. The target atom is described by a central potential [5], such as the Hartree-Fock-Slater potential with the exchange term omitted [6]. Of course, as the photon energy decreases, and the kinetic energy of the created electron (or positron) becomes very low, the calculations based on this independent-particle model cease to be quantitative and give only a qualitative guide to features.

We use the same formalism we used for the atomic-field bremsstrahlung calculation [7]. Following our previous bremsstrahlung work [7], we write the pair-production cross section, differential with respect to positron energy E_+ and to positron and electron angles as

$$d\sigma/dE_+d\Omega_+d\Omega_-=(2\pi)^{-5}p_-E_-p_+E_+|M_{fi}|^2 . \quad (1)$$

Here the pair-production matrix element is

$$M_{fi}=(2\pi\alpha/k)^{1/2}\int d^3x\,\psi_2^\dagger(\mathbf{p}_-,\mathbf{r},\zeta_-)\times\boldsymbol{\alpha}\cdot\boldsymbol{\epsilon}\psi_1(-\mathbf{p}_+,\mathbf{r},\zeta')e^{i\mathbf{k}\cdot\mathbf{r}} . \quad (2)$$

The photons are specified by momentum $\mathbf{k}$, energy k, and photon polarization vector $\boldsymbol{\epsilon}$ such that

$$\boldsymbol{\epsilon}^*\cdot\boldsymbol{\epsilon}=1,\quad \boldsymbol{\epsilon}\cdot\mathbf{k}=0 . \quad (3)$$

Here $\psi_2(\mathbf{p}_-,\mathbf{r},\zeta_-)$ is the electron wave function asymptotically normalized to a unit-amplitude plane wave (or distorted plane wave in the point-Coulomb case) of four-momentum $(E_-,\mathbf{p}_-)$ and four polarization $(0,\zeta_-)$ in its rest frame plus an incoming spherical wave; the positron wave function contains asymptotically spherical incoming waves, as the substitutions $E_1\rightarrow-E_+$, $\mathbf{p}_1\rightarrow-\mathbf{p}_+$ (but $|\mathbf{p}_1|\rightarrow|\mathbf{p}_+|$), and $\zeta_1\rightarrow\zeta'=\zeta_+-2\hat{p}_+(\hat{p}_+\cdot\zeta_+)$ change outgoing into incoming spherical waves, namely,

$$i\gamma^2\psi_+^{\text{in}*}(\mathbf{p}_+,\mathbf{r},\zeta_+)=\psi_1^{\text{out}}(-\mathbf{p}_+,\mathbf{r},\zeta') , \quad (4)$$

where ψ_+ is the positron wave function. That is [8],

$$\left.\begin{matrix}\psi_1(\mathbf{p},\mathbf{r},\zeta)\\ \psi_2(\mathbf{p},\mathbf{r},\zeta)\end{matrix}\right\}=4\pi\sum_{\kappa m}[\Phi_{\kappa m}^\dagger(\hat{p})\chi(\zeta)]i^l e^{\{\pm\}i\delta_\kappa}\psi_{\kappa m}(\mathbf{r}) , \quad (5)$$

where

$$\psi_{\kappa m}(\mathbf{r})=r^{-1}\begin{bmatrix}g_\kappa(r)\Phi_{\kappa m}(\hat{\mathbf{r}})\\ if_\kappa(r)\Phi_{-\kappa m}(\hat{\mathbf{r}})\end{bmatrix} , \quad (6)$$

and

$$\Phi_{\kappa m}(\hat{\mathbf{r}})=\sum_{s=\pm1/2}C(l\tfrac{1}{2}j;m-s,s)Y_{l,m-s}(\hat{\mathbf{r}})\chi^s \quad (7)$$

is an eigenstate of J^2, J_z, and L^2. The angular momentum operator is $\mathbf{J}=\mathbf{L}+\mathbf{S}$, the quantity $C(l\frac{1}{2}j;m-s,s)$ is the Clebsch-Gordan coefficient, and the quantum number $\kappa=\mp(j+\frac{1}{2})$ as $j=l\pm\frac{1}{2}$. The radial wave functions g_κ and f_κ satisfy the radial Dirac equations

$$\begin{aligned} dg_\kappa(r)/dr &= (p_0+1-V)f_\kappa(r)-\kappa g_\kappa(r)/r \ , \\ df_\kappa(r)/dr &= -(p_0-1-V)g_\kappa(r)+\kappa f_\kappa(r)/r \ , \end{aligned} \tag{8}$$

with $p_0=-E_+$ for ψ_1 and $p_0=E_-$ for ψ_2, where V is the central potential described by the target atom. We use the spinor representation for Dirac electron and positron wave functions. In this representation any matrix element between four-component states may be reduced to matrix elements between two-component spinors

$$\chi=c_{1/2}\chi^{1/2}+d_{1/2}\chi^{-1/2} \tag{9}$$

with

$$\chi^{1/2}=\begin{bmatrix}1\\0\end{bmatrix}, \quad \chi^{-1/2}=\begin{bmatrix}0\\1\end{bmatrix} \tag{10}$$

and

$$\chi^+\chi=1 \ . \tag{11}$$

Choosing a coordinate system centered at the atomic nucleus with the z axis along $\mathbf{k}$, $\hat{y}$ along $\mathbf{k}\times\mathbf{p}_+$, and $\hat{x}$ in the $(\mathbf{k},\mathbf{p}_+)$ plane, and inserting Eqs. (5) into Eq. (2), we obtain

$$\begin{aligned} M_{fi} &= 16\pi^2(2\pi\alpha/k)^{1/2} \\ &\times \sum_{\kappa_1,m_1,\kappa_2,m_2} [\Phi_2^\dagger(\hat{p}_-)\chi_2]^\dagger[\Phi_1^\dagger(-\hat{p}_+)\chi_1] \\ &\times(-1)^{l_1}e^{i(\delta_{\kappa_1}+\delta_{\kappa_2})} \\ &\times[\epsilon_-R_+(m_2)+\epsilon_+R_-(m_2)] \ , \end{aligned} \tag{12}$$

where

$$\begin{aligned} R_\pm(m_2) &= R^\pm_{\kappa_2\kappa_1}(m_2)\delta_{m_1,m_2\mp1} \ , \\ R^\pm_{\kappa_2\kappa_1}(m) &= \sum_{n=1}^{2} Q_n^\pm(m)\sum_l{}' P_n^\pm(m)s_n \ . \end{aligned} \tag{13}$$

The index l runs from $|l_2'-l_1|$ to $(l_2'+l_1)$ in steps of 2 for $n=1$, and from $|l_2-l_1'|$ to (l_2+l_1') in steps of 2 for $n=2$. Here

$$\epsilon_\pm=\epsilon_x\pm i\epsilon_y \ ; \tag{14}$$

$$l'=l+\eta_k, \quad \eta_\kappa=-\kappa/|\kappa| \ ; \tag{15}$$

$$\begin{aligned} Q_1^\pm(m) &= \eta_{\kappa_2}(-1)^{m\mp1/2}[(2l_2'+1)(2l_1+1)]^{1/2} \\ &\times C^\pm_{-\kappa_2,m}C^\mp_{\kappa_1,m\mp1} \ , \\ Q_2^\pm(m) &= -\eta_{\kappa_1}(-1)^{m\mp1/2}[(2l_2+1)(2l_1'+1)]^{1/2} \\ &\times C^\pm_{\kappa_2,m}C^\mp_{-\kappa_1,m\mp1} \ ; \end{aligned} \tag{16}$$

TABLE I. Comparisons of unpolarized pair-production cross section $\sigma(E_+)=[Z^{-2}d\sigma/dE_+]_{\text{unpol}}$ for $k=2.10m_ec^2$; $Z=1$, 13, and 82; $y=(E_+-1)/(k-2)=0.1$, 0.3, 0.5, 0.7, 0.9, and 0.95 between results of Øverbø, Mork, and Olsen ($\sigma_{\text{ØMO}}$) for the point-Coulomb potential, our results calculated with the partial-wave method for the point-Coulomb potential (σ_C) and for Hartree-Fock-Slater potential with the exchange term omitted (σ_{HFN}), the results calculated with the energy-shift screening theory (σ_{EST}), and the results calculated with the corrected-effective normalization screening theory (σ_{CNST}). Here the cross section $\sigma(E_+)$ are in units of $\mu b/m_ec^2$, and $a[n]$ shall mean $a\times10^n$.

Z	y	$\sigma_{\text{ØMO}}$	σ_C	σ_{HFN}	$\sigma_{\text{HFN}}/\sigma_C$	$\sigma_{\text{CNST}}/\sigma_{\text{HFN}}$	$\sigma_{\text{EST}}/\sigma_{\text{HFN}}$
1	0.1	0.920	0.9265	0.9279	1.00	1.00	1.00
	0.3	1.50	1.517	1.517	1.00	1.00	1.00
	0.5	1.69	1.693	1.693	1.00	1.00	1.00
	0.7	1.58	1.585	1.584	0.999	1.00	1.00
	0.9	1.10	1.102	1.101	0.999	1.00	0.999
	0.95	0.850	0.8509	0.8487	0.997	1.00	1.00
13	0.1	0.220	0.2211	0.3184	1.44	1.00	0.997
	0.3	1.21	1.222	1.318	1.08	1.00	1.01
	0.5	1.95	1.944	2.001	1.03	1.00	1.00
	0.7	2.32	2.329	2.353	1.01	1.00	1.00
	0.9	2.46	2.462	2.470	1.00	1.00	1.00
	0.95	2.49	2.483	2.501	1.01	1.00	0.997
82	0.1		6.554[−8]	1.108[−3]	1.69[4]	1.03	8.95
	0.3		4.153[−3]	0.1079	26.0	1.01	1.48
	0.5	0.115	0.1156	0.7043	6.09	1.00	1.11
	0.7	0.650	0.6486	2.115	3.26	0.997	1.03
	0.9	1.92	1.909	4.420	2.32	0.996	
	0.95	2.36	2.356	5.128	2.18	0.996	

TABLE II. Same as Table I, except for $k=2.01m_ec^2$ and $Z=1$, 6, and 13.

Z	y	$\sigma_{\text{ØMO}}$	σ_C	σ_{HFN}	$\sigma_{\text{HFN}}/\sigma_C$	$\sigma_{\text{CNST}}/\sigma_{\text{HFN}}$	$\sigma_{\text{EST}}/\sigma_{\text{HFN}}$
1	0.1	0.008 15	0.008 111	0.008 331	1.03	1.00	1.00
	0.3	0.016 0	0.016 03	0.016 12	1.01	1.00	1.00
	0.5	0.019 3	0.019 25	0.019 28	1.00	1.00	1.00
	0.7	0.019 3	0.019 29	0.019 25	0.998	1.00	1.00
	0.9	0.015 3	0.015 45	0.015 31	0.991	1.00	1.00
	0.95	0.013 3	0.013 33	0.013 13	0.985	1.00	1.00
6	0.1	0.000 76	0.000 758 6	0.002 539	3.35	0.983	1.50
	0.3	0.009 80	0.009 821	0.013 55	1.38	0.970	1.02
	0.5	0.021 3	0.021 20	0.024 80	1.17	1.00	1.01
	0.7	0.031 5	0.031 45	0.034 56	1.10	0.963	1.01
	0.9	0.040 4	0.040 37	0.043 62	1.08	0.961	0.997
	0.95	0.042 4	0.042 55	0.046 27	1.09	0.960	
13	0.1		7.166[−6]	6.890[−4]	96.2	1.03	2.41
	0.3	0.001 9	0.001 911	0.008 460	4.43	1.01	1.20
	0.5	0.010 5	0.010 52	0.024 08	2.29	1.00	1.05
	0.7	0.025 8	0.025 84	0.044 77	1.73	0.998	1.01
	0.9	0.045 8	0.045 80	0.068 44	1.49	0.995	
	0.95	0.051 0	0.051 29	0.074 87	1.46	0.994	

$$P_1^{\pm}(m)=(-1)^{(l_2'+l_1-l)/2}T(l_2',l_1,l;m\mp\tfrac{1}{2}) ,$$
$$P_2^{\pm}(m)=(-1)^{(l_2+l_1'-l)/2}T(l_2,l_1',l;m\mp\tfrac{1}{2}) ; \tag{17}$$

$$T(l_2,l_1,l;m)=(2l+1)\begin{bmatrix} l_2 & l_1 & l \\ 0 & 0 & 0 \end{bmatrix}\begin{bmatrix} l_2 & l_1 & l \\ -m & m & 0 \end{bmatrix} ; \tag{18}$$

$$C^{\pm}_{\kappa,m}=C(l\tfrac{1}{2}j;m\mp\tfrac{1}{2},\pm\tfrac{1}{2}) ; \tag{19}$$

and

$$s_1=\int_0^{\infty}dr\, j_l(kr)g_{\kappa_1}f_{\kappa_2} ,$$
$$s_2=\int_0^{\infty}dr\, j_l(kr)g_{\kappa_2}f_{\kappa_1} . \tag{20}$$

To calculate the pair-production cross section $d\sigma/dE_+d\Omega_+d\Omega_-$ from Eq. (1), we need $|M_{fi}|^2$, which can be obtained from Eq. (12). To obtain the unpolarized pair-production cross section $[d\sigma/dE_+d\Omega_+d\Omega_-]_{\text{unpol}}$ we average the $d\sigma/dE_+d\Omega_+d\Omega_-$ over the initial-photon polarizations and summed over the final electron and positron spins. Integrating the unpolarized pair-production cross section $[d\sigma/dE_+d\Omega_+d\Omega_-]_{\text{unpol}}$ over the positron and electron angles $d\Omega_+$ and $d\Omega_-$, we obtain the unpolarized pair-production positron energy spectrum

$$\sigma(E_+)\equiv[Z^{-2}d\sigma/dE_+]_{\text{unpol}}$$
$$=\lambda_0\sum_{\kappa_2,\kappa_1,m=|m_2|}\{[R^+_{\kappa_2\kappa_1}(m)]^2+[R^-_{\kappa_2\kappa_1}(m)]^2\} , \tag{21}$$

TABLE III. Same as Table I, except for $k=2.001m_ec^2$, $Z=1$ and 6, and the cross section $\sigma(E_+)$ are in units of nb/m_ec^2.

Z	y	$\sigma_{\text{ØMO}}$	σ_C	σ_{HFN}	$\sigma_{\text{HFN}}/\sigma_C$	$\sigma_{\text{CNST}}/\sigma_{\text{HFN}}$	$\sigma_{\text{EST}}/\sigma_{\text{HFN}}$
1	0.1	0.033	0.032 74	0.051 33	1.57	1.02	0.999
	0.3	0.135	0.135 0	0.149 4	1.11	1.01	1.01
	0.5	0.208	0.208 4	0.216 9	1.04	1.00	1.01
	0.7	0.253	0.254 5	0.257 4	1.01	1.01	1.01
	0.9	0.272	0.272 1	0.274 3	1.01	0.997	1.00
	0.95	0.276	0.276 6	0.282 1	1.02	1.00	0.989
6	0.1		9.937[−6]	1.048[−2]	1055.0	17.5	4.40
	0.3		2.196[−3]	0.105 5	48.0	1.03	1.31
	0.5	0.0268	0.026 89	0.305 8	11.4	1.00	0.980
	0.7	0.102	0.103 2	0.593 3	5.75	0.996	
	0.9	0.244	0.244 5	0.950 9	3.89	0.989	
	0.95	0.290	0.290 3	1.05 6	3.64	0.987	

where

$$\lambda_0=\frac{32\alpha}{Z^2k}p_-E_-p_+E_+ , \tag{22}$$

and $R^{\pm}_{\kappa_2\kappa_1}(m)$ are given by Eqs. (13). Integrating the unpolarized pair-production cross section $[d\sigma/dE_+d\Omega_+d\Omega_-]_{\text{unpol}}$ over the electron angle $d\Omega_-$, we obtain

$$\sigma(E_+,\theta_+)=[Z^{-2}d\sigma/dE_+d\Omega_+]_{\text{unpol}}$$
$$=\lambda_0\sum_{\kappa_2,\kappa_1,\bar{\kappa}_1}(-1)^{\bar{l}_1+l_2}\cos\delta\sum_{m=|m_2|}B(m) , \tag{23}$$

where

$$B(m)=A^{+}_{+}(m)\bar{A}^{+}_{+}(m)+A^{+}_{-}(m)\bar{A}^{+}_{-}(m)$$
$$+A^{-}_{+}(m)\bar{A}^{-}_{+}(m)+A^{-}_{-}(m)\bar{A}^{-}_{-}(m) , \tag{24}$$

$$\delta=\delta_{\kappa_1}-\delta_{\bar{\kappa}_1} , \tag{25}$$

$$A^{\pm}_{\pm}(m)=C^{\pm}_{\kappa_1,m-1}Y_{l_1,m-1\mp1/2}(\hat{p}_1)R^{+}_{\kappa_2\kappa_1}(m) , \tag{26}$$

$$A^{\pm}_{\mp}(m)=C^{\pm}_{\kappa_1,m+1}Y_{l_1,m+1\mp1/2}(\hat{p}_1)R^{-}_{\kappa_2\kappa_1}(m) , \tag{27}$$

where the bar over $A^{\pm}_{\pm}$ corresponds to $\bar{\kappa}_1$.

The problem of calculating the unpolarized pair-production cross sections $\sigma(E_+)$ and $\sigma(E_+,\theta_+)$ has been reduced to computing $R^{\pm}_{\kappa_2\kappa_1}(m)$. We used the similar numerical method we used for our relativistic bremsstrahlung calculations [7]. The $Q^{\pm}_n(m)$ and $P^{\pm}_n(m)$ factors present no great problem. Electron and positron wave functions are obtained in partial-wave series by numerically solving the radial Dirac equation. The radial integrals s_n are calculated numerically to the point where the continuum wave functions of electrons and positrons can be approximately considered as the modified phase-shifted free field wave functions and an integration by parts method can be used. Then the rest of the radial integrals were calculated by the integration by parts method analytically.

With the partial-wave method we have obtained the positron energy spectra of pair production $\sigma(E_+)=[Z^{-2}d\sigma/dE_+]_{\text{unpol}}$ for incident photons of energy $k=2.001$, 2.01, and 2.10 m_ec^2, for the elements of atomic number $Z=1$, 6, 13, and 82. These calculated results are shown in Tables I–III and Figs. 1–3. Here the unpolarized pair-production cross sections are calculated numerically both with the Hartree-Fock-Slater potential with the exchange term omitted [6] (HFN potential) and the point-Coulomb potential. In Tables I–III we show comparisons of unpolarized pair-production cross section $\sigma(E_+)=[Z^{-2}d\sigma/dE_+]_{\text{unpol}}$ in the field of atomic nucleus between the results of Øverbø, Mork, and Olsen for the point-Coulomb potential $\sigma_{\text{ØMO}}$ calculated with the analytic partial-wave method [1] and our results σ_C calculated with the numerical partial-wave method also for the point-Coulomb potential. The agreement is very good. This provides a check of our numerical calculation. In Figs. 1–3 we also show comparisons of our $\sigma_C(E_+)$ with the results calculated by the Born approximation [9]; we see that the Born approximation is not

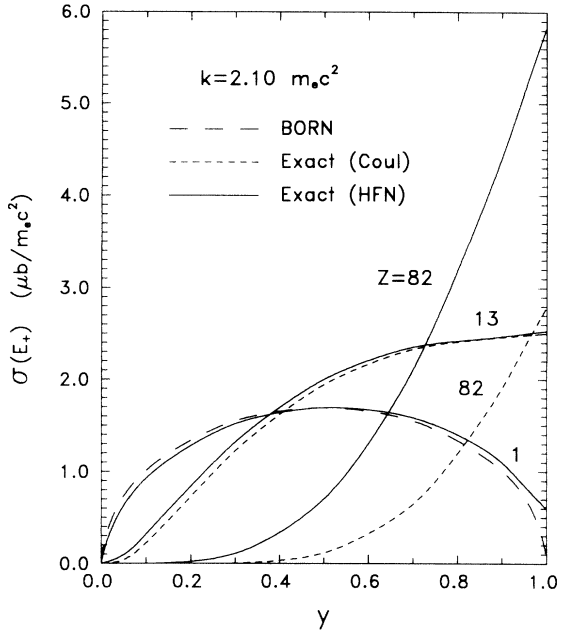

FIG. 1. Pair-production differential cross section $\sigma(E_+)=[Z^{-2}d\sigma/dE_+]_{\text{unpol}}$ of the exact relativistic numerical calculation in partial waves for the HFN potential (solid line) and the point-Coulomb potential (Coul, short-dashed line) and of the calculation by the Born approximation (Born, long-dashed line) for $Z=1$, 13, and 82 and $k=2.10m_ec^2$.

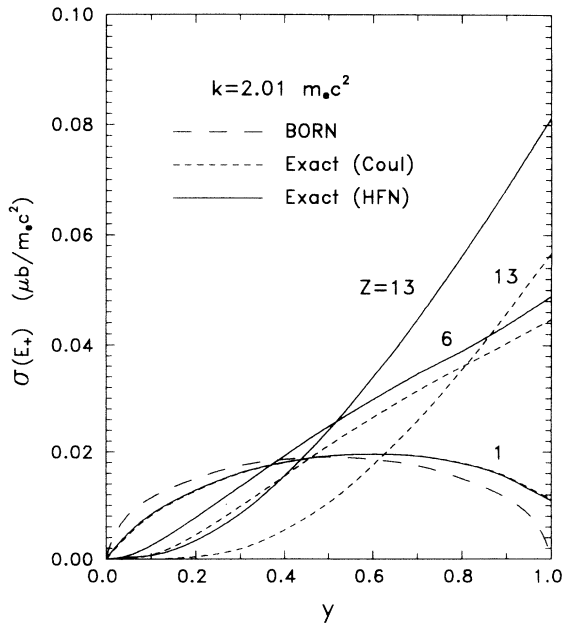

FIG. 2. Same as Fig. 1, except for $k=2.01m_ec^2$ and $Z=1$, 6, and 13.

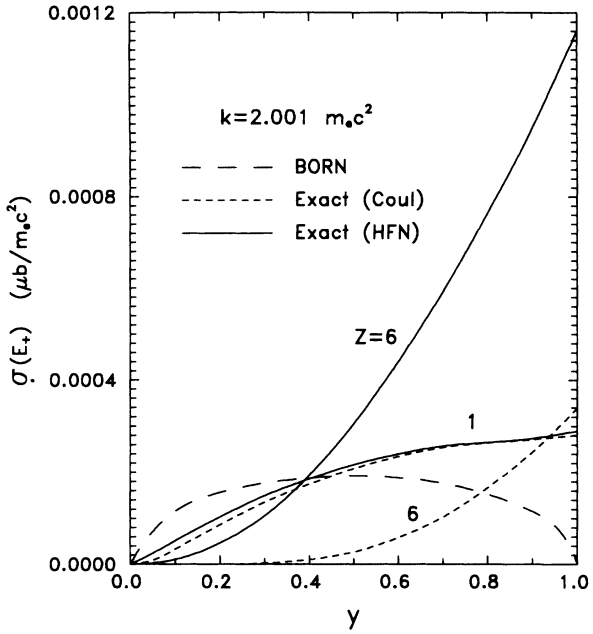

FIG. 3. Same as Fig. 1, except for $k=2.001m_ec^2$ and $Z=1$ and 6.

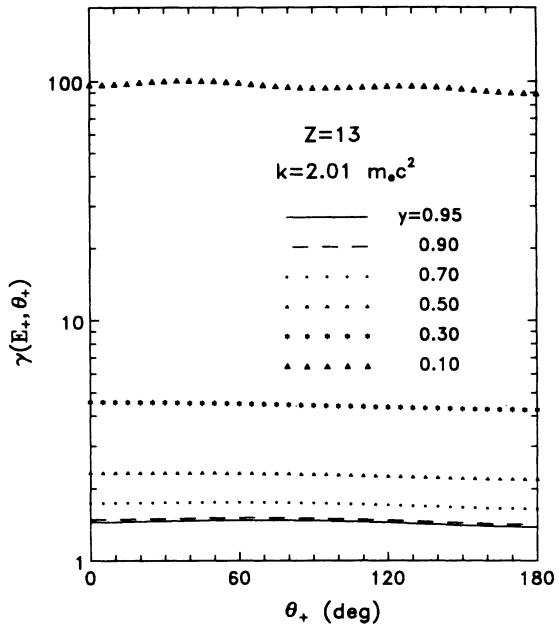

FIG. 5. Pair-production screening factors $\gamma(E_+,\theta_+)$ for $Z=13$, $k=2.01m_ec^2$, and $y=0.1,0.3,0.5,0.7,0.9,0.95$.

good in this low-photon-energy region, as expected [1].

Our results in Tables I–III or Figs. 1–3 show that the atomic-electron screening effect increases as Z increases, k decreases, and E_+ decreases. The ratio $\sigma_{\rm HFN}/\sigma_C$ varies from 0.985 to 1.69×10^4. When the screening effect is important [10], it increases the cross section $\sigma(E_+)$. This is because the atomic electrons decrease the Coulomb repulsion of the positrons (which is responsible for the asymmetric positron energy distribution) [3].

In Tables I–III we also show comparisons of our results $\sigma_{\rm HFN}$ with the results calculated with the energy-shift screening theory ($\sigma_{\rm EST}$) [3], i.e., there is a simple relation between screening and point-Coulomb pair-production energy distributions for a given photon energy k:

$$\sigma_S(E_+ + V_0, E_- - V_0) = \sigma_C(E_+, E_-) \,. \tag{28}$$

Our results indicate that the approximate treatment of screening through energy-shift screening theory is good for $Z=1$ with $V_0=-3.65\times10^{-5}m_ec^2$ for $k=2.10m_ec^2$ down to $2.001m_ec^2$. For $Z=6$ and $k=2.01m_ec^2$ with $V_0=-7.20\times10^{-4}m_ec^2$, the energy-shift screening theory is good, except for small $y=(E_+-1)/(k-2)$, where the screening effect is important. For $Z=6$ and

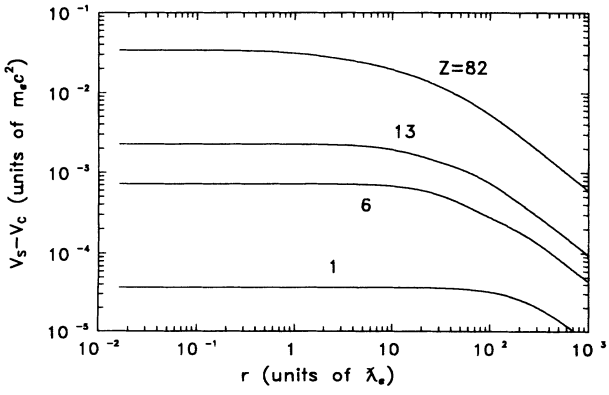

FIG. 4. Difference V_S-V_C between the screened (HFN) and the point-Coulomb potential as a function of distance r, in units of the Compton electron wavelength $\lambda\!\!\!^{-}_e$.

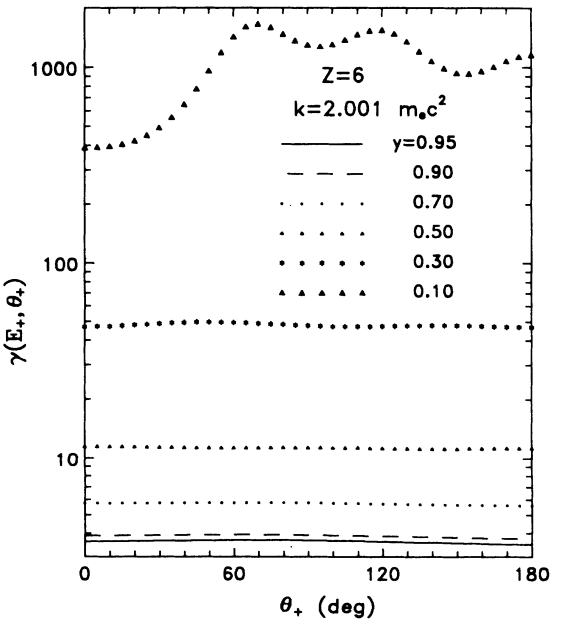

FIG. 6. Same as Fig. 5, except for $Z=6$ and $k=2.001m_ec^2$.

$k=2.001m_ec^2$, the energy-shift screening theory works better by choosing $V_0=-4.60\times10^{-4}m_ec^2$, but it is still poor. In this case, the screening effect is very important. Similar conclusions are reached for higher Z elements. As Z increases and k decreases, the EST works better by a proper choice of V_0. However, since the screening effect is very important, the EST is not adequate. This can be understood qualitatively from Fig. 4, where we show the potential difference V_S-V_C between the screened (HFN) and the point-Coulomb potential. The difference remains the same from small distances to quite large distances for low Z elements only.

In Figs. 5 and 6 we show the corresponding screening factor $\gamma(E_+,\theta_+)$, the ratio of screened to point-Coulomb angular cross sections $\sigma(E_+,\theta_+)$. We see that the shapes of angular distributions are almost independent of screening. This suggests that the atomic-electron screening is primarily a normalization effect. In Tables I–III we show comparisons of our results $\sigma_{\rm HFN}$ with the results calculated with the corrected-effective normalization screening theory ($\sigma_{\rm CNST}$). It indicates that the CNST is good for the cases we considered in this paper, except for $Z=6$, $k=2.001m_ec^2$, and $y=0.1$. This can be understood qualitatively from Fig. 6, where $\gamma(E_+,\theta_+)$ varies with θ_+ irregularly for the case with $y=0.1$.

This work was support in part by the National Science Council, Republic of China, under Grants Nos. NSC 82-0208-M-008-010 and NSC 83-0208-M-008-026.

[1] O. Øverbø, K. J. Mork, and H. A. Olsen, Phys. Rev. **175**, 1978 (1968); Phys. Rev. A **8**, 668 (1973); I. Øverbø, Ph.D. thesis, University of Trondheim, 1970; J. W. Motz, H. A. Olsen, and H. W. Koch, Rev. Mod. Phys. **41**, 581 (1969).

[2] J. C. Jaeger and H. R. Hulme, Proc. R. Soc. London Ser. A **153**, 443 (1936); J. C. Jaeger, Nature **137**, 781 (1936); **148**, 86 (1941).

[3] H. K. Tseng and R. H. Pratt, Phys. Rev. A **4**, 1835 (1971); **6**, 2049 (1972); **21**, 454 (1980); **24**, 1127 (1981). Unrationalized units are used throughout, i.e., $\hbar=m_e=c=1$, unless otherwise specified.

[4] F. T. Avignone III and Ali E. Khalil, Phys. Rev. A **24**, 2920 (1981).

[5] R. H. Pratt, in *Fundamental Processes in Energetic Atomic Collisions,* edited by H. O. Lutz, J. S. Briggs, and H. Kleinpoppen (Plenum, New York, 1983), p. 150.

[6] D. A. Liberman, J. B. Mann, and J. T. Waber, Comput. Phys. Commun. **2**, 107 (1971).

[7] H. K. Tseng and R. H. Pratt, Phys. Rev. A **3**, 100 (1971).

[8] See, for example, H. A. Olsen, in *Applications of Quantum Electrodynamics,* edited by G. Höhler, Springer Tracts in Modern Physics Vol. 44 (Springer, Berlin, 1968).

[9] H. A. Bethe and W. Heitler, Proc. R. Soc. London Ser. A **146**, 83 (1934); F. Sauter, Ann. Phys. (Leipzig) **20**, 404 (1934); G. Racah, Nuovo Cimento **11**, 461 (1934); **11**, 467 (1934).

[10] Unfortunately, there are no experimental results available for unpolarized pair-production cross sections $\sigma(E_+)$ and $\sigma(E_+,\theta_+)$ at these low-energy cases to make comparisons with our calculated results. The status of experimental work on the pair-production cross section to 1981 has been summarized by Motz, Olsen, and Koch (see Ref. [1]), by Øverbø, Mork, and Olsen (see Ref. [1]), by Tseng and Pratt (see Ref. [3]), and by Avignone and Khalil (see Ref. [4]).